Polymer 186 (2020) 122030

Contents lists available at ScienceDirect

Polymer

journal homepage: http://www.elsevier.com/locate/polymer

Enhanced electrical and electromagnetic interference shielding properties of uniformly dispersed carbon nanotubes filled composite films via solvent-free process using ring-opening polymerization of cyclic butylene terephthalate

Ji-un Jang [a], Ji Eun Cha [b], Seung Hwan Lee [c], Jaewoo Kim [b], Beomjoo Yang [d], Seong Yun Kim [c,*], Seong Hun Kim [a,**]

[a] Department of Organic and Nano Engineering, Hanyang University, 222 Wangsimni-ro, Haengdang-dong, Seongdong-gu, Seoul, 04763, Republic of Korea
[b] Multifunctional Structural Composite Research Center, Institute of Advanced Composite Materials, Korea Institute of Science and Technology (KIST), 92 Chudong-ro, Bongdong-eup, Wanju-gun, Jeonbuk, 55324, Republic of Korea
[c] Division of Polymer-Nano & Textile Engineering, Chonbuk National University, 567 Baekje-daero, Deokjin-gu, Jeonju-si, Jeonbuk, 54896, Republic of Korea
[d] School of Civil Engineering, Chungbuk National University, 1 Chungdae-ro, Seowon-gu, Cheongju-si, Chungbuk, 28644, Republic of Korea

ARTICLE INFO

Keywords:
Cyclic butylene terephthalate
Composite
Carbon nanotube

ABSTRACT

In order to develop a nanocomposite film based on multi-walled carbon nanotubes (MWCNTs) as an electromagnetic wave shielding material, we propose a solvent-free melting process for fabricating highly dispersed MWCNT-filled polymer composite films with high electrical conductivity and electromagnetic interference (EMI)-shielding properties. By observing aggregates (particles larger than 0.7 μm) using X-ray micro-computed tomography (micro-CT), the uniform dispersion of the MWCNT fillers in the composite films was confirmed. Furthermore, the electrical conductivity and EMI shielding effectiveness (SE) values calculated using percolation and Simon's equations, respectively, were confirmed to agree with experimental data, indicating excellent MWCNT dispersion. The fabricated composites exhibited excellent electrical conductivity, EMI SE, and EMI specific SE (SSE) values of 4.33 S/cm, 30 dB, and of 24.8 $dBcm^3g^{-1}$, respectively, and the EMI SSE value was as good as metal levels. The proposed solvent-free process can be contributed to the commercialization of EMI SE composite films based on MWCNTs.

1. Introduction

Equipment malfunction due to electromagnetic waves arising from the integration of electronic devices has recently attracted significant attention in the electronics industry [1]. To overcome the problem, electromagnetic wave shielding materials are widely applied. In these materials, the main mechanisms of the EMI SE are absorption and reflection. Absorption of electromagnetic waves is caused by interaction with electrical (or magnetic) dipoles [1,2]. Electromagnetic wave reflection is due to the interaction of incident electromagnetic waves with mobile charges, such as electrons [1–3]. Transmitted electromagnetic waves can undergo multiple reflections that are repeatedly absorbed or reflected on the surfaces of the shielding material [1–3].

EMI SE is affected by various physical properties of the shielding material, such as dielectric permittivity, magnetic permeability and electrical conductivity [2,3]. To develop a high-performance EMI shielding material, many studies [3–5] have been performed on high electrical conductivity. In general, metals such as copper and aluminum are selected as EMI shielding materials [4,5]. Meanwhile, because the development of light-weight EMI shielding materials is desirable, various studies [4–7] on polymer-based EMI SE materials have been performed to achieve an excellent EMI SSE.

Polymers have advantages in terms of SSE due to their low density, but are unsuitable for use as shielding materials because of their low electrical conductivity [8–12]. The electrical conductivity of polymers can be improved by incorporating carbon nanotube (CNT), a

* Corresponding author.
** Corresponding author.
E-mail addresses: sykim82@jbnu.ac.kr (S.Y. Kim), kimsh@hanyang.ac.kr (S.H. Kim).

https://doi.org/10.1016/j.polymer.2019.122030
Received 18 August 2019; Received in revised form 18 November 2019; Accepted 23 November 2019
Available online 29 November 2019
0032-3861/

nanomaterial known to have a large aspect ratio and excellent electrical conductivity [13–19]. The electrical conductivity of nanocomposites incorporating CNTs is known to be influenced by the shape, size and dispersion of the filler [18–24]. In particular, the filler dispersion is a main determinant of electrical properties based on the electron tunnel effect and percolation theory [25–28]. Many studies [29–32] have been performed to enhance the CNT dispersion chemically and physically. Despite various strategies [31–35] have been developed to inhibit the aggregation of CNTs, such as surfactant dispersion, chemical treatment of CNTs, and polymer wrapping, they are difficult to apply in the composite industry because of the high process cost and low productivity.

Methods for enhancing the dispersion of nanocarbon filler using *in situ* polymerizable resins, such as ϵ-caprolactam and cyclic butylene terephthalate (CBT), have been reported due to promote an easy and rapid manufacturing process and low process cost [36–41]. Resins composed of monomers or oligomers exhibiting a low melt viscosity enhance the CNT dispersion and induce polymer wrapping by *in situ* polymerization [38,42,43]. In this study, the fabrication of an EMI SE film incorporating MWCNT using an *in situ* polymerizable cyclic oligoester was proposed, and the electrical properties and EMI SE of the fabricated composite were evaluated based on theoretical calculations.

2. Experimental

2.1. Materials

MWCNT (Jenotube 8, JEIO, Incheon, Korea) was used as a filler to improve the electrical conductivity of the composite films. The filler used was a one-dimensional carbon allotrope with bundle length and single strand diameter of 100–200 μm and 7–10 nm, respectively. The defect level (ID/IG) of MWCNT (details in Supplementary material) was 1.34 as shown in Fig. S1. CBT (CBT 160, Cyclics® Co., Schenectady, NY, USA) was used as the matrix of the composite films. CBT is a cyclic oligomer composed of 2–7 butyl monomers with low molecular weight (M_w) of $(220)_n$ (n = 2–7) g/mol [44]. CBT exhibited melt and flow characteristics at 130–150 °C. When heated above 160 °C, it was polymerized to poly (butylene terephthalate) (pCBT) by the contained catalyst (butyltin chloride dihydroxide, FASCAT 4101, Arkema GmbH, Düsseldorf, Germany) of 3 mol‰. The mechanism of ring-opening polymerization of CBT has been widely investigated and reported as shown in Fig. S2 [45].

2.2. Composite fabrication

The raw materials were dried at 80 °C for 12 h to remove moisture before composite fabrication. To achieve good MWCNT dispersion, the milled CBT and MWCNTs were weighed out at the target ratio, and then mixed using a mixing machine (ARE 310, Thinky Corp., Tokyo, Japan) at 2000 rpm for 3 min, as shown in Fig. 1 and supplementary video. The mixture was heated using a hot press (D3P-20J, Dae Heung Science, Incheon, Korea) under 300 psi at 230 °C for 20 min. The composition and thickness of the fabricated composites are summarized in Table 1.

Supplementary video related to this article can be found at https://doi.org/10.1016/j.polymer.2019.122030.

2.3. Characterization

2.3.1. Crystalline structure

Wide-angle X-ray diffraction (WAXD) measurements were performed using an X-ray diffractometer (PANalytical X'Pert Pro, Malvern Panalytical Ltd., Royston, UK) equipped with a Giono-meter PW3050/60 working with Cu K alpha radiation (1.54 Å). The diffraction intensity was recorded by continuous scanning at a rate of 0.02 deg/s over a range of $10 < 2\theta < 60$ deg (θ = Bragg angle).

2.3.2. Thermal behavior

Thermal behaviors of CBT, pCBT and the fabricated composites were measured using differential scanning calorimetry (DSC, Q20, TA Instrument, DE, USA) with nitrogen. The fabricated composites were heated from 50 to 250 °C at a rate of 10 °C/min and maintained at 250 °C for 5 min. The samples were subsequently cooled to 50 °C at a rate of 10 °C/min. DSC analysis was performed by repeating the above cycle twice. Crystallization temperature (T_{c1}, T_{c2}), crystallization enthalpy (ΔH_{c1}, ΔH_{c2}), melt temperature (T_{m1}, T_{m2}) and melt enthalpy (ΔH_{m1}, ΔH_{m2}) obtained in the 1st and 2nd cycles of each sample are listed in Table 2. The degree of crystallinity (X_c) was calculated by the following equation [46].

$$X_c(\%) = \frac{\Delta H_{m2}}{(1-b) \times \Delta H_m^0} \times 100 \quad (1)$$

where ΔH_m^0 is the melt enthalpy of ideal crystalline structure of pCBT (85.75 J/g [47]), and b is the filler content of composite film.

2.3.3. Morphology

The diameter and bundle length of the MWCNT, and the fracture surface of the composite film were observed using a field emission scanning electron microscope (FE-SEM, Nova NanoSEM 450, FEI Co., Hillsboro, OR, USA). The fabricated composites were fractured after freezing in liquid nitrogen. The fractured surfaces of composites were coated with platinum under vacuum using a sputtering coating machine (Ion Sputter E−1030, Hitachi High Technologies Co., Tokyo, Japan) for

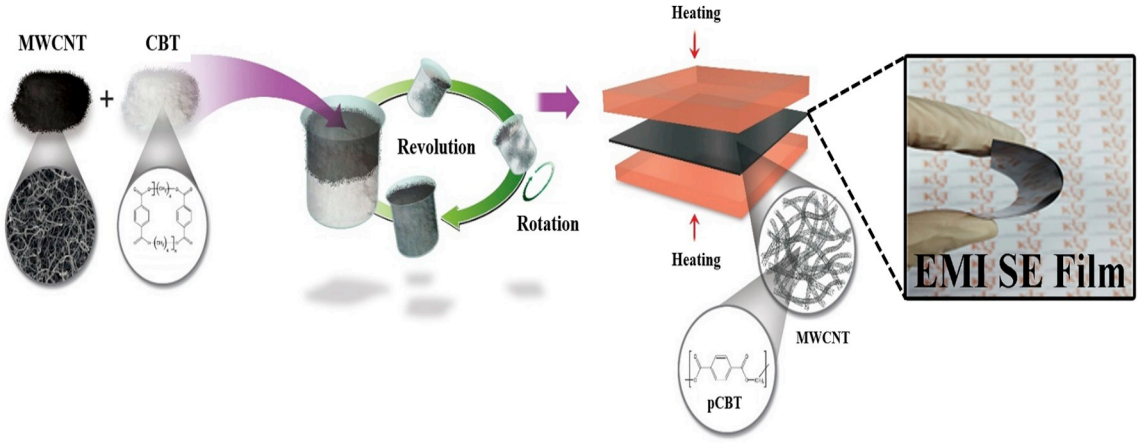

Fig. 1. Schematic of one-step solvent-free process using particle mixing and *in situ* polymerization for fabrication of EMI SE composite film incorporating uniformly dispersed MWCNTs.

Table 1
Composition and thickness of fabricated composites.

Filler content (Sample code)	0 wt% (pCBT)	0.5 wt% (pCBT/MWCNT 0.5 wt%)	1 wt% (pCBT/MWCNT 1 wt%)	3 wt% (pCBT/MWCNT 3 wt%)	5 wt% (pCBT/MWCNT 5 wt%)	7 wt% (pCBT/MWCNT 7 wt%)
CBT (g)	30	29.85	29.70	29.10	28.50	27.90
MWCNT (g)	0	0.15	0.30	0.90	1.50	2.10
Specimen thickness (t) (mm)	0.56	0.60	0.65	0.65	1.03	1.20

Table 2
DSC data of the crystallization and melting process for the composites.

Sample code	1st heating		1st cooling		2nd heating		2nd cooling		X_c (%)
	T_{m1}(°C)	ΔH_{m1}(J/g)	T_{c1}(°C)	ΔH_{c1}(J/g)	T_{m2}(°C)	ΔH_{m2}(J/g)	T_{c2}(°C)	ΔH_{c2}(J/g)	
CBT	141.03	73.61	185.92	52.91	221.37	54.81	185.94	51.19	63.92
pCBT	226.59	53.52	190.14	51.98	223.21	55.51	188.10	49.65	64.73
pCBT/MWCNT 7 wt%	218.78	54.44	199.40	51.22	222.93	54.38	197.79	48.78	68.10

120 s. The coated specimens were observed under a nitrogen vacuum at a current of 10 kV. The three-dimensional (3D) internal structure of the prepared composite film was observed using micro-computed tomography (micro-CT, Skyscan 1172, Bruker Co., Billerica, MA, USA) with a resolution of 0.7 μm.

2.3.4. Electrical conductivity

The electrical conductivity of the fabricated composite films was measured using the four-probe method according to ASTM D 257 (FPP-RS8, DASOL ENG, Cheongju, Korea) and an ultrahigh resistance meter (SM-8220, HIOKI E. E. Corporation, Nagano, Japan) under ambient conditions.

2.3.5. EMI SE

The EMI SE was measured at room temperature in the frequency range of 100 kHz−3 GHz using a WILTRON 54169A scalar measurement system (Anritsu, Pine Brook, NJ, USA) according to ASTM D4935-10.

3. Theoretical approaches

The electrical conductivity and EMI SE values of the fabricated composites were compared with the theoretical values derived using the percolation equation and Simon's equation, respectively [48–51].

3.1. Percolation equation

A common feature of all percolation systems is that the conductive component is randomly distributed and intergranular resistances are randomly present between the conductive particles or regions. Based on the randomly dispersed conductive components, the general percolation behavior depends on the critical volume fraction (ϕ_c) and the percolation exponent (s and v), which are affected by the uniformity of the polymer thickness on the conductive filler surface. By applying the critical exponents to the Bruggeman symmetric media equation, the normalized standard percolation result is expressed [52]. The electrical conductivity of the polymer composite incorporated with MWCNT can generally be described as [52]:

$$\sigma_c = \sigma_m\left[(\phi_c)/(\phi_c - \phi_f)\right]^s \quad (if,\ \phi_f < \phi_c)$$

$$\sigma_c = \sigma_f\left[(\phi_f - \phi_c)/(1 - \phi_c)\right]^v \quad (if,\ \phi_f > \phi_c) \tag{2}$$

where σ_c, σ_m, and σ_f are the electrical conductivity of the composite, matrix and filler, respectively. In addition, ϕ_f and ϕ_c denote the volume fraction of filler and percolation threshold (the onset of the transition, vol%). Superscripts of s and v signify the universal exponent and the universal critical exponent that is depending on the uniformity of the polymer thickness on the MWCNT surface. In the present study, we adopted the material properties in accordance with [53,54] as: $\sigma_m = 1.39 \cdot 10^{-13}$ S/cm, $\sigma_f = 1 \cdot 10^2$ S/cm [53], and $\phi_c = 0.62$ vol% [54] (density of MWCNT = 2.1 g/cm^3 [28], density of pCBT = 1.3 g/cm^3 [55]). The model parameters were fixed as s = 1 and v = 1.02 in this study.

3.2. Simon's equation

Simon's equation is a useful method for evaluating the EMI SE values of polymer matrix-based composites [50]. The total shielding effect (SE_{total}) is determined by absorption (A), reflection (R) and multiple reflection (B) ($SE_{total} = SE_A + SE_R + SE_B$). The main factors affecting EMI SE are electromagnetic wave frequency, material size, and electrical conductivity. In particular, electrical conductivity is known to be an important factor because it can enhance the reflection effect of the EMI SE mechanism due to the interaction between mobile charge carriers (holes or electrons) and the electromagnetic field. Assuming multiple reflections (B) are ignored, the EMI SE of composites incorporating a conductive filler is expressed by the following equation [50].

$$SE(dB) = 50 + 10\log_{10}(\sigma / f) + 1.7t(\sigma f)^{1/2} \tag{3}$$

where, σ: electrical conductivity of composite (S/cm), f: frequency (MHz), f = 100 − 3000 (MHz), t: sample thickness (cm), the first two terms are due to the reflection effect of the composite (R), and the last term is determined by the absorption effect (A).

4. Results and discussion

It is necessary to check whether the CBT molecules are well converted to pCBT in the composite film because the ring-opening polymerization of CBT molecules can be inhibited by the MWCNTs. The Fourier transform infrared (FT-IR) spectra of the fabricated composites are shown in the Fig. S3 (details in Supplementary material). Characteristic peaks were observed around 1714 cm^{-1} (C═O), 1118 cm^{-1} (C–O aliphatic end) and 1103 cm^{-1} (C–O aromatic end) due to ester group of CBT, pCBT and the prepared composites [56]. However, since the same functional group was shown before and after the ring-opening polymerization of CBT, it was difficult to determine whether the matrix was polymerized due to the slight differences in the peaks [43]. WAXD patterns of CBT, pCBT, and pCBT/MWCNT are shown in Fig. 2a. The crystalline peaks observed for the CBT resin showed that the CBT resin was composed of crystalline oligoesters of 2–7 monomers. (010), (100) and (11^{-}1) crystalline peaks that were absent in the WAXD pattern of CBT were identified in the WAXD pattern of pCBT, indicating that the CBT molecules have been well converted to pCBT polymers [57–60]. In

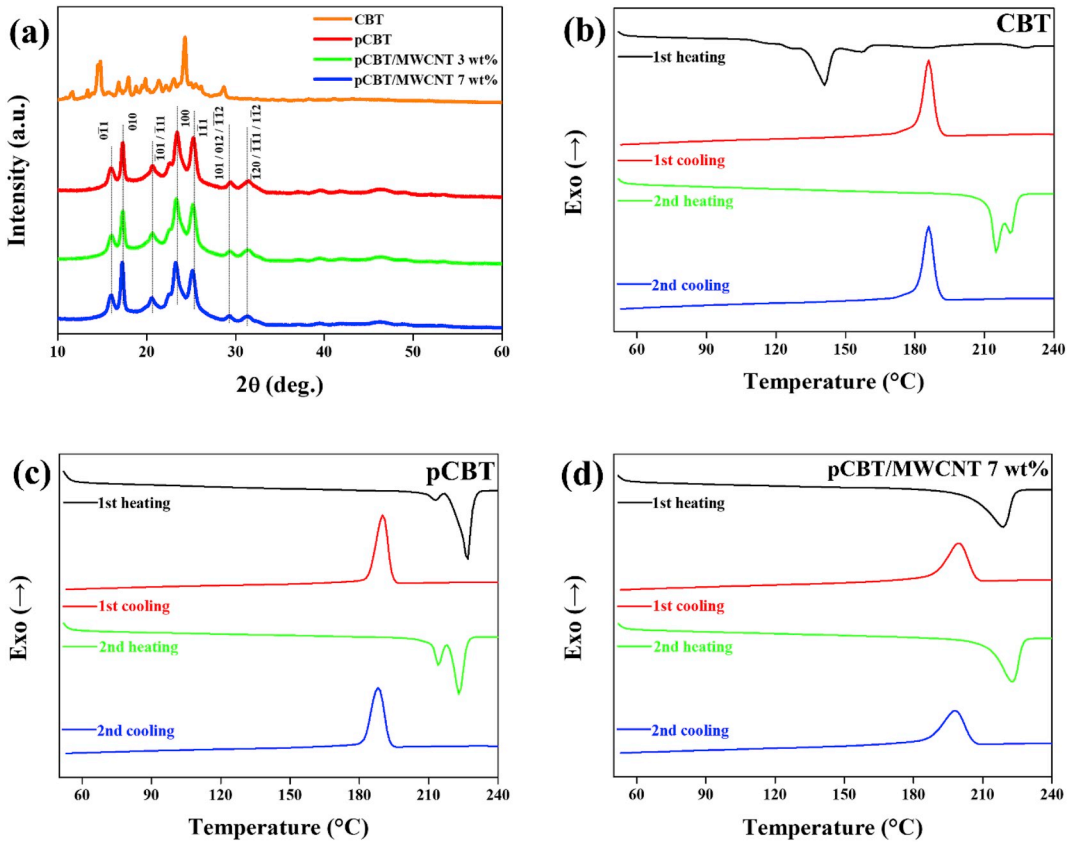

Fig. 2. (a) WAXD results of the CBT, pCBT and composite film fabricated by the proposed process and DSC thermograms of (b) CBT, (c) pCBT and (d) pCBT/MWCNT 7 wt% composite fabricated by the proposed process.

the WAXD pattern of the pCBT/MWCNT composite films, those peaks were also clear observed. From the similar WAXD patterns of pCBT and the composites incorporating MWCNT of 3 and 7 wt%, the interference effect of MWCNTs on the polymerization of CBT can be neglected.

DSC analysis is another method for determining the polymerization of CBT resin [47,58]. The thermal behavior of the prepared CBT, pCBT and pCBT/MWCNT was measured using DSC as shown in Fig. 2b–d and Table 2. In the 1st heating cycle of CBT (Fig. 2b), an endothermic peak was observed at 130–150 °C due to the melting of CBT [47,58]. An exothermic peak was found at about 185.92 °C due to the crystallization of the pCBT melt during the 1st cooling cycle of CBT. In the 2nd heating cycle, no endothermic peak was observed in the temperature range of 130–150 °C because the CBT oligomer was polymerized *in situ* to pCBT during the 1st heating [47,58]. Therefore, the second DSC curve of CBT was similar to the DSC curve of pCBT (Fig. 2c) [58]. In the 1st and 2nd heating cycles of pCBT, endothermic peaks due to melting of pCBT were observed at about 225 °C. The observed double melting behavior may be due to melting and recrystallization of the incomplete crystalline structure of pCBT [47,58]. In the 1st and 2nd cooling cycles, an exothermic peak corresponding to the crystallization of the molten pCBT appeared at about 188.10 °C [61]. An exothermic peak was observed at about 197.79 °C in the cooling curve of the pCBT/MWCNT composite (Fig. 2d), which was relatively higher than that of pCBT. It has already been reported that MWCNT acted as a nucleating agent that promotes crystallization [61]. Except for the melt enthalpy of CBT (73.61 J/g) in the 1st heating cycle as shown in Table 2, the melt and crystallization enthalpy obtained from CBT, pCBT and the fabricated composites were determined in the range of 53.52–55.51 J/g and 48.78–52.91 J/g, respectively. Compared to those of CBT and pCBT, degree of crystallinity (X_c) of pCBT/MWCNT 7 wt% sample were increased about 4% due to the incorporation of fillers [62]. Therefore, the results of WAXD and DSC confirmed that the CBT oligomers in the composites were polymerized to the pCBT polymers during the composite fabrication.

The FE-SEM images of the single strand diameter, bundle length of the MWCNT and the fracture surface of the pCBT/MWCNT composite film according to the filler weight fraction produced by the proposed process are shown in Fig. 3a–d. A uniform dispersion was observed at the fracture surface of the composite incorporating 7 wt% or less MWCNT. Analysis by FE-SEM was limited due to the two-dimensional and local observations [36,63,64]. Filler aggregates of size 700 nm or larger inside the large area (~50 mm^3) of MWCNT composites can be analyzed by micro-CT. Non-destructive and 3D analysis of the samples was performed using micro-CT as shown in Fig. 3e and f. Filler aggregation was rarely observed in the composite fabricated using the proposed process. Therefore, MWCNTs were uniformly dispersed by the one-step solvent-free process.

The electrical conductivity of the composite film fabricated by the proposed process according to the weight fraction of MWCNT is shown in Fig. 4. Due to the high aspect ratio and excellent electrical conductivity (>10^2 S/cm) of the MWCNT, an efficient conductive network was formed inside the composite, and percolation behavior appeared before the MWCNT content was 1 wt%. The composite incorporating 7 wt% MWCNT exhibited enhanced electrical conductivity (4.33 S/cm) by 13 orders of magnitude on the logarithmic scale compared to the electrical conductivity of pCBT (1.39×10^{-13} S/cm). In addition, the measured electrical conductivity was confirmed to be almost the same as the electrical conductivity calculated based on the percolation equation. This meant that the measured electrical conductivities of the composites approached the theoretical values obtained by the percolation equation due to the uniform dispersion of the MWCNTs confirmed above. Comparisons of filler content and electrical conductivity of MWCNT filled composites prepared by melt mixing process are shown in Supplementary material (Fig. S4).

EMI SE is known to be proportional to the electrical conductivity of

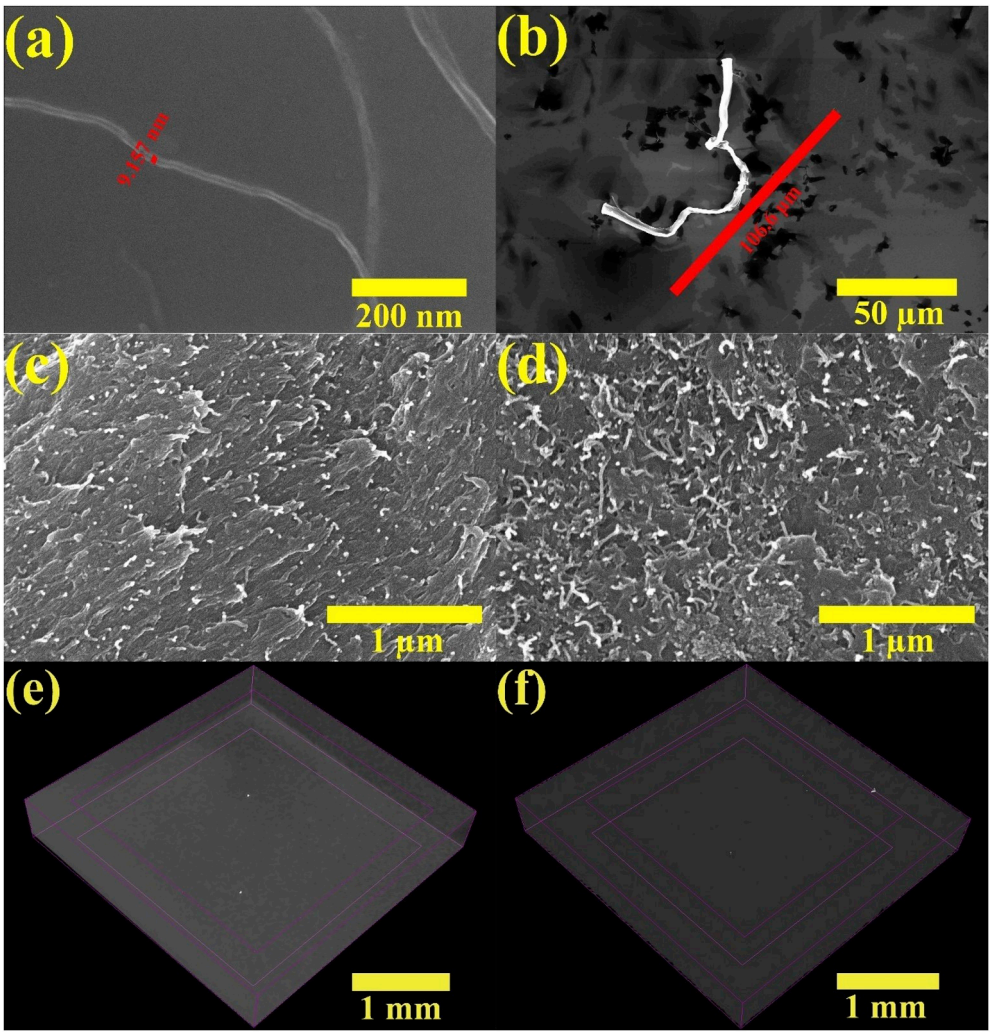

Fig. 3. (a) Single strand diameter and (b) bundle length of MWCNT used for composite film fabrication, and FE-SEM images of fracture surfaces of the prepared composite films incorporating MWCNT of (c) 3 wt% and (d) 7 wt%, and micro-CT images of the prepared composite films incorporating MWCNT of (e) 3 wt% and (f) 7 wt%.

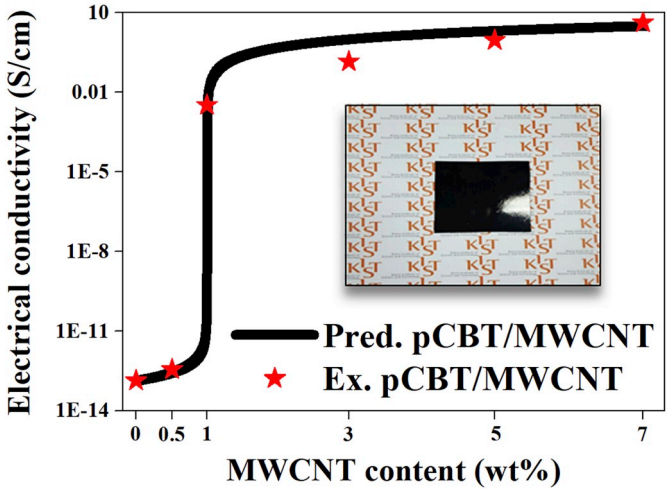

Fig. 4. Experimentally measured and theoretically calculated electrical conductivities of the composite films.

conductive materials due to the reflection mechanism of electromagnetic waves [1,2]. The composite film fabricated by the proposed process exhibited an EMI SE value of 3 dB at 1 wt% MWCNT incorporation and increased to 30 dB at 7 wt% MWCNT, as shown in Fig. 5. The minimum value calculated using Simon's equation according to electromagnetic wave frequency was similar to the experimental value. Furthermore, the EMI SE of the prepared samples was in agreement with the value calculated according to the MWCNT content. These results implied that the value of the composite material approached the expected value based on the volume resistivity (the inverse value of the electrical conductivity). As a result, the electrical conductivity and EMI SE values of the pCBT/MWCNT composite films fabricated using the proposed process were improved with increasing filler content, and were close to predictions by the percolation and Simon 's equation based on filler dispersion.

Metals such as copper, aluminum, and stainless steel are typical materials used for EMI SE [6]. Although they exhibit excellent EMI SE due to high electrical conductivity, it is difficult to apply metals as light-weight materials because of their high density. Therefore, it is necessary to consider the SSE value which associates the density of the material with the EMI SE. The SSE of the prepared pCBT/MWCNT composite film incorporating a filler content of 7 wt% was 24.8 $dBcm^3g^{-1}$, which is much higher than the EMI SSE values of 10 and 11 $dBcm^3g^{-1}$ reported by Shui et al. for bulk copper and stainless steel,

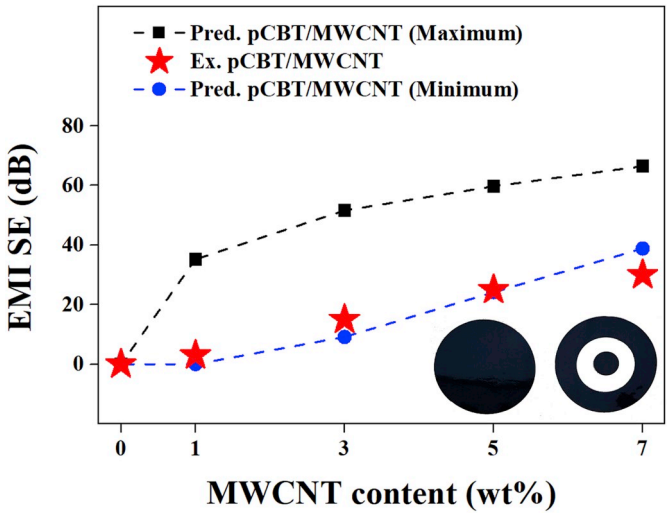

Fig. 5. Experimentally measured and theoretically calculated EMI SE of the composite films.

respectively [7]. It was also confirmed that the EMI SE value of the film manufactured by the proposed process was higher than that of aluminum foil (24.4 $dBcm^{-3}g^{-1}$) reported by Shahzad et al. [51]. Consequently, the fabricated film can be applied to the EMI SE light-weight material industry instead of metals.

5. Conclusion

The fabrication of a composite film incorporating uniformly dispersed MWCNT using a one-step and solvent-free melt process was proposed. Based on non-destructive 3D analysis using micro-CT, it was observed that the composites fabricated by the proposed process showed excellent MWCNT dispersion. The electrical conductivity and EMI values of the fabricated composites were compared with the values calculated using percolation and Simon's equations, respectively. The agreement between the measured and calculated values confirmed that the proposed process induced excellent dispersion of the nanocarbon filler in the fabricated composites. In addition, the SSE value of the fabricated EMI SE film was higher than those of some typical metals, indicating that it can be applied as a light-weight material in the EMI SE industry. In conclusion, the one-step process capable of uniformly dispersing the nanocarbon filler without solvents can contribute to the commercialization of excellent electrical conductivity and EMI SE composite film.

Author contributions

Ji-un Jang: Writing - Original Draft. Ji Eun Cha: Investigation. Seung Hwan Lee: Visualization. Jaewoo Kim: Resources. Beomjoo Yang: Formal analysis. Seong Yun Kim: Supervision, Conceptualization, Writing - Review & Editing. Seong Hun Kim: Project administration, Methodology.

Declaration of competing interest

The authors declare no competing interest.

Acknowledgments

This research was supported by Chonbuk National University in 2018 under "Research Base Construction Fund Support Program", and was partially supported by Basic Science Research Program (2017R1C1B5077037 and 2016R1A6A1A03013422) through the National Research Foundation of Korea (NRF) funded by the Ministry of Education, and the Industrial Technology Innovation Program (10082586) funded by the Ministry of Trade, Industry & Energy of Korea.

Appendix A. Supplementary data

Supplementary data to this article can be found online at https://doi.org/10.1016/j.polymer.2019.122030.

References

[1] C.R. Paul, Introduction to Electromagnetic Compatibility, Wiley and Sons Inc., Hoboken, 2006.
[2] D.D.L. Chung, Electromagnetic interference shielding effectiveness of carbon materials, Carbon 39 (2001) 279–285.
[3] M.H. Al-Saleh, U. Sundararaj, Electromagnetic interference shielding mechanisms of CNT/polymer composites, Carbon 47 (2009) 1738–1746.
[4] G.A. Gelves, M.H. Al-Saleh, U. Sundararaj, Highly electrically conductive and high performance EMI shielding nanowire/polymer nanocomposites by miscible mixing and precipitation, J. Mater. Chem. 21 (2011) 829–836.
[5] D.D.L. Chung, Materials for electromagnetic interference shielding, J. Mater. Eng. Perform. 9 (2000) 350–354.
[6] S. Geetha, K.K. Satheesh Kumar, C.R.K. Rao, M. Vijayan, D.C. Trivedi, EMI shielding: methods and materials—a review, J. Appl. Polym. Sci. 112 (2009) 2073–2086.
[7] X. Shui, D.D.L. Chung, Nickel filament polymer-matrix composites with low surface impedance and high electromagnetic interference shielding effectiveness, J. Electron. Mater. 26 (1997) 928–934.
[8] I. Manners, Polymers and the periodic table: recent developments in inorganic polymer science, Angew. Chem. Int. Ed. 35 (1996) 1602–1621.
[9] M. Najafi, R. Ansari, A. Darvizeh, Effect of cryogenic aging on nanophased fiber metal laminates and glass/epoxy composites, Polym. Compos. 40 (2019) 2523–2533.
[10] D.R. Son, A.V. Raghu, K.R. Reddy, H.M. Jeong, Compatibility of thermally reduced graphene with polyesters, J. Macromol. Sci. Part B: Phys. 55 (2016) 1099–1110.
[11] K.R. Reddy, K.V. Karthik, S.B.B. Prasad, S.K. Soni, H.M. Jeong, A.V. Raghu, Enhanced photocatalytic activity of nanostructured titanium dioxide/polyaniline hybrid photocatalysts, Polyhedron 120 (2016) 169–174.
[12] K.R. Reddy, K.-P. Lee, A.I. Gopalan, Self-assembly directed synthesis of poly (ortho-toluidine)-metal (gold and palladium) composite nanospheres, J. Nanosci. Nanotechnol. 7 (2007) 3117–3125.
[13] K.R. Reddy, B.C. Sin, K.S. Ryu, J.-C. Kim, H. Chung, Y. Lee, Conducting polymer functionalized multi-walled carbon nanotubes with noble metal nanoparticles: synthesis, morphological characteristics and electrical properties, Synth. Met. 159 (2009) 595–603.
[14] Y.-P. Zhang, S.-H. Lee, K.R. Reddy, A.I. Gopalan, K.-P. Lee, Synthesis and characterization of core-shell SiO2 nanoparticles/poly(3-aminophenylboronic acid) composites, J. Appl. Polym. Sci. 104 (2007) 2743–2750.
[15] K.R. Reddy, K.-P. Lee, A.I. Gopalan, Novel electrically conductive and ferromagnetic composites of poly(aniline-co-aminonaphthalenesulfonic acid) with iron oxide nanoparticles: synthesis and characterization, J. Appl. Polym. Sci. 106 (2007) 1181–1191.
[16] M. Hassan, K.R. Reddy, E. Haque, S.N. Faisal, S. Ghasemi, A.I. Minett, V.G. Gomes, Hierarchical assembly of graphene/polyaniline nanostructures to synthesize free-standing supercapacitor electrode, Compos. Sci. Technol. 98 (2014) 1–8.
[17] J. Liang, Y. Wang, Y. Huang, Y. Ma, Z. Liu, J. Cai, C. Zhang, H. Gao, Y. Chen, Electromagnetic interference shielding of graphene/epoxy composites, Carbon 47 (2009) 922–925.
[18] E.T. Thostenson, Z. Ren, T.W. Chou, Advances in the science and technology of carbon nanotubes and their composites: a review, Compos. Sci. Technol. 61 (2001) 1899–1912.
[19] R.H. Baughman, A.A. Zakhidov, W.A. De Heer, Carbon nanotubes–the route toward applications, Science 297 (2002) 787–792.
[20] K.R. Reddy, K.-P. Lee, A.I. Gopalan, A.M. Showkat, Facile synthesis of hollow spheres of sulfonated polyanilines, Polym. J. 38 (2006) 349–354.
[21] K.R. Reddy, K.-P. Lee, Y. Lee, A.I. Gopalan, Facile synthesis of conducting polymer–metal hybrid nanocomposite by in situ chemical oxidative polymerization with negatively charged metal nanoparticles, Mater. Lett. 62 (2008) 1815–1818.
[22] Y.R. Lee, S.C. Kim, H.-i. Lee, H.M. Jeong, A.V. Raghu, K.R. Reddy, B.K. Kim, Graphite oxides as effective fire retardants of epoxy resin, Macromol. Res. 19 (2011) 66–71.
[23] K.R. Reddy, K.P. Lee, A.I. Gopalan, Self-assembly approach for the synthesis of electro-magnetic functionalized Fe3O4/polyaniline nanocomposites: effect of dopant on the properties, Colloids Surf., A 320 (2008) 49–56.
[24] K.R. Reddy, H.M. Jeong, Y. Lee, A.V. Raghu, Synthesis of MWCNTs-core/thiophene polymer-sheath composite nanocables by a cationic surfactant-assisted chemical oxidative polymerization and their structural properties, J. Polym. Sci., Part A: Polym. Chem. 48 (2010) 1477–1484.
[25] S. Kirkpatrick, Percolation and conduction, Rev. Mod. Phys. 45 (1973) 574–588.

[26] A.L. Efros, B.I. Shklovskii, Critical behaviour of conductivity and dielectric constant near the metal-non-metal transition threshold, Phys. Status Solidi B Basic Res. 76 (1976) 475–485.
[27] S.Y. Kim, Y.J. Noh, J. Yu, Prediction and experimental validation of electrical percolation by applying a modified micromechanics model considering multiple heterogeneous inclusions, Compos. Sci. Technol. 106 (2015) 156–162.
[28] B.J. Yang, J.-u. Jang, S.-H. Eem, S.Y. Kim, A probabilistic micromechanical modeling for electrical properties of nanocomposites with multi-walled carbon nanotube morphology, Compos. Appl. Sci. Manuf. 92 (2017) 108–117.
[29] T. Saito, K. Matsushge, K. Tanaka, Chemical treatment and modification of multi-walled carbon nanotubes, Phys. B 323 (2002) 280–283.
[30] P.-C. Ma, N.A. Siddiqui, G. Marom, J.-K. Kim, Dispersion and functionalization of carbon nanotubes for polymer-based nanocomposites: a review, Compos. Appl. Sci. Manuf. 41 (2010) 1345–1367.
[31] M. Park, H. Lee, J.-u. Jang, J.H. Park, C.H. Kim, S.Y. Kim, J. Kim, Phenyl glycidyl ether as an effective noncovalent functionalization agent for multiwalled carbon nanotube reinforced polyamide 6 nanocomposite fibers, Compos. Sci. Technol. 177 (2019) 96–102.
[32] X.-L. Xie, Y.-W. Mai, X.-P. Zhou, Dispersion and alignment of carbon nanotubes in polymer matrix: a review, Mater. Sci. Eng. R Rep. 49 (2005) 89–112.
[33] A.I. Zhbanov, E.G. Pogorelov, Y.C. Chang, Van der Waals interaction between two crossed carbon nanotubes, ACS Nano 4 (2010) 5937–5945.
[34] L. Vaisman, H.D. Wagner, G. Marom, The role of surfactants in dispersion of carbon nanotubes, Adv. Colloid Interface Sci. 128–130 (2006) 37–46.
[35] A. Satake, Y. Miyajima, Y. Kobuke, Porphyrin−carbon nanotube composites formed by noncovalent polymer wrapping, Chem. Mater. 17 (2005) 716–724.
[36] J.-u. Jang, H.S. Lee, J.W. Kim, S.Y. Kim, S.H. Kim, I. Hwang, B.J. Kang, M.K. Kang, Facile and cost-effective strategy for fabrication of polyamide 6 wrapped multi-walled carbon nanotube via anionic melt polymerization of ε-caprolactam, Chem. Eng. J. 373 (2019) 251–258.
[37] S.Y. Kim, Y.J. Noh, J. Yu, Thermal conductivity of graphene nanoplatelets filled composites fabricated by solvent-free processing for the excellent filler dispersion and a theoretical approach for the composites containing the geometrized fillers, Compos. Appl. Sci. Manuf. 69 (2015) 219–225.
[38] H.S. Kim, J.H. Kim, C.-M. Yang, S.Y. Kim, Synergistic enhancement of thermal conductivity in composites filled with expanded graphite and multi-walled carbon nanotube fillers via melt-compounding based on polymerizable low-viscosity oligomer matrix, J. Alloy. Comp. 690 (2017) 274–280.
[39] L. Tzounis, T. Gärtner, M. Liebscher, P. Pötschke, M. Stamm, B. Voit, G. Heinrich, Influence of a cyclic butylene terephthalate oligomer on the processability and thermoelectric properties of polycarbonate/MWCNT nanocomposites, Polymer 55 (2014) 5381–5388.
[40] H. Chen, C. Huang, W. Yu, C. Zhou, Effect of thermally reduced graphite oxide (TrGO) on the polymerization kinetics of poly(butylene terephthalate) (pCBT)/TrGO nanocomposites prepared by in situ ring-opening polymerization of cyclic butylene terephthalate, Polymer 54 (2013) 1603–1611.
[41] P. Fabbri, E. Bassoli, S.B. Bon, L. Valentini, Preparation and characterization of poly (butylene terephthalate)/graphene composites by in-situ polymerization of cyclic butylene terephthalate, Polymer 53 (2012) 897–902.
[42] S.Y. Kim, Y.J. Noh, J. Yu, Improved thermal conductivity of polymeric composites fabricated by solvent-free processing for the enhanced dispersion of nanofillers and a theoretical approach for composites containing multiple heterogeneities and geometrized nanofillers, Compos. Sci. Technol. 101 (2014) 79–85.
[43] J.-u. Jang, H.C. Park, H.S. Lee, M.S. Khil, S.Y. Kim, Electrically and thermally conductive carbon fibre fabric reinforced polymer composites based on Nanocarbons and an in-situ Polymerizable cyclic Oligoester, Sci. Rep. 8 (2018) 7659.
[44] Z. Jiang, S. Siengchin, L.-M. Zhou, M. Steeg, J. Karger-Kocsis, H.C. Man, Poly (butylene terephthalate)/silica nanocomposites prepared from cyclic butylene terephthalate, Compos. Appl. Sci. Manuf. 40 (2009) 273–278.
[45] T. Abt, M. Sánchez-Soto, A review of the recent advances in cyclic butylene terephthalate technology and its composites, Crit. Rev. Solid State Mater. Sci. 42 (2017) 173–217.
[46] S.Y. Kim, S.H. Kim, J.Y. Kim, H.H. Cho, Novel CO_2 laser drawing of thermotropic liquid crystal polymer and poly(ethylene 2,6-naphthalate) blend fibers, J. Appl. Polym. Sci. 104 (2007) 205–211.
[47] Z.A.M. Ishak, K.G. Gatos, J. Karger-Kocsis, On the in-situ polymerization of cyclic butylene terephthalate oligomers: DSC and rheological studies, Polym. Eng. Sci. 46 (2006) 743–750.
[48] D.S. McLachlan, Equation for the conductivity of metal-insulator mixtures, J. Phys. C Solid State Phys. 18 (1985) 1891.
[49] D.S. McLachlan, M. Blaszkiewicz, R.E. Newnham, Electrical resistivity of composites, J. Am. Ceram. Soc. 73 (1990) 2187–2203.
[50] R.M. Simon, EMI shielding through conductive plastics, Polym. Plast. Technol. Eng. 17 (1981) 1–10.
[51] F. Shahzad, M. Alhabeb, C.B. Hatter, B. Anasori, S.M. Hong, C.M. Koo, Y. Gogotsi, Electromagnetic interference shielding with 2D transition metal carbides (MXenes), Science 353 (2016) 1137–1140.
[52] D.S. McLachlan, Analytical functions for the dc and ac conductivity of conductor-insulator composites, J. Electroceram. 5 (2000) 93–110.
[53] G. Xu, Q. Zhang, W. Zhou, J. Huang, F. Wei, The feasibility of producing MWCNT paper and strong MWCNT film from VACNT array, Appl. Phys. A Mater. 92 (2008) 531–539.
[54] S. Stankovich, D.A. Dikin, G.H.B. Dommett, K.M. Kohlhaas, E.J. Zimney, E. A. Stach, Graphene-based composite materials, Nature 442 (2006) 282–286.
[55] Z.A.M. Ishak, Y.W. Leong, M. Steeg, J. Karger-Kocsis, Mechanical properties of woven glass fabric reinforced in situ polymerized poly(butylene terephthalate) composites, Compos. Sci. Technol. 67 (2007) 390–398.
[56] A.R. Tripathy, W.J. Macknight, S.N. Kukureka, In-situ copolymerization of cyclic poly(butylene terephthalate) oligomers and ε-caprolactone, Macromolecules 37 (2004) 6793–6800.
[57] M. Harsch, J. Karger-Kocsis, A. Apostolov, Crystallization-induced shrinkage, crystalline, and thermomechanical properties of in situ polymerized cyclic butylene terephthalate, J. Appl. Polym. Sci. 108 (2008) 1455–1461.
[58] Y.J. Noh, S. Lee, S.Y. Kim, J.R. Youn, High-speed fabrication of thermoplastic carbon fiber fabric composites with a polymerizable, low-viscosity cyclic butylene terephthalate matrix for automotive applications, Macromol. Res. 22 (2014) 528–533.
[59] D. Xu, J. Karger-Kocsis, A.A. Apostolov, Hybrids from HNBR and in situ polymerizable cyclic butylene terephthalate (CBT): structure and rolling wear properties, Eur. Polym. J. 45 (2009) 1270–1281.
[60] C.-M. Wu, C.-W. Huang, Melting and crystallization behavior of copolymer from cyclic butylene terephthalate and polycaprolactone, Polym. Eng. Sci. 51 (2011) 1004–1013.
[61] D. Wu, L. Wu, G. Yu, B. Xu, M. Zhang, Crystallization and thermal behavior of multiwalled carbon nanotube/poly (butylenes terephthalate) composites, Polym. Eng. Sci. 48 (2008) 1057–1067.
[62] F. Wu, G. Yang, Synthesis and properties of poly(butylene terephthalate)/multiwalled carbon nanotube nanocomposites prepared by in situ polymerization and in situ compatibilization, J. Appl. Polym. Sci. 118 (2010) 2929–2938.
[63] H.S. Kim, J.-u. Jang, J. Yu, S.Y. Kim, Thermal conductivity of polymer composites based on the length of multi-walled carbon nanotubes, Compos. B Eng. 79 (2015) 505–512.
[64] H.G. Jang, B.J. Yang, M.-S. Khil, S.Y. Kim, J. Kim, Comprehensive study of effects of filler length on mechanical, electrical, and thermal properties of multi-walled carbon nanotube/polyamide 6 composites, Compos. Appl. Sci. Manuf. 125 (2019) 105542.